

COMPARISON OF FRICTION MODELS IN THE JOINTS OF AN EXPERIMENTAL MANIPULATOR WITH 3-DOF

TOMAS CAKURDA¹, MONIKA TROJANOVA¹, ALEXANDER HOSOVSKY¹, PAVLO POMIN¹

¹Technical University of Kosice, Faculty of Manufacturing Technologies with the Seat in Presov, Slovakia

DOI: 10.17973/MMSJ.2023_12_2023069

tomas.cakurda@tuke.sk

The article is devoted to the identification of friction in the joints of a 3-DOF manipulator with fluidic muscles. For the identification of friction, four different models were proposed, namely linear friction model, extended friction model, non-linear friction model and LuGre model. The values of the coefficients of the proposed models were estimated in the Matlab Simulink program environment based on the comparison of the measured and simulated curves of the angle of rotation of individual joints. The corresponding friction models with adjusted values of their coefficients were validated using two statistical indicators, namely Root Mean Square Error and Sum Square Error. The validation process consisted of comparing the measured and simulated course of the rotation angle of the joint using the corresponding estimated friction model. The aim of the validation was to compare the performance of individual friction models and to choose the most optimal variant for the dynamic model of the investigated system.

KEYWORDS

Experimental manipulator, Friction models, Estimation, Validation

1 INTRODUCTION

Currently, research in the field of performance of robot manipulators is an essential element for effective control of robots. The process of identifying individual parameters enables the creation of reliable dynamic models of the respective systems. The dynamic model is used as a tool for improving position management, determining optimal trajectories due to energy savings, safety of the system itself and safe interaction with a person or work environment [Garabin 2020, Matheson 2019]. Among the dynamic parameters of robotic manipulators, we include weights, positions of centres of gravity, moments of inertia and identification of friction in individual joints. Parameters that cannot be determined by measurement are obtained by creating a dynamic model, performing experiments on a real system and then comparing measured and simulated values to determine the optimal values of the parameters sought [Hao 2021].

The identification of friction in joints is an essential step in creating a dynamic model of a real system. Industrial applications that place a high emphasis on precise position control require accurate identification of friction in individual joints of robotic manipulators. Friction in robotic systems is a complex phenomenon that contains many non-linear aspects. Friction itself arises from the relative movement of two surfaces that are in contact with each other. Friction depends on the

shape of the contact surfaces, the roughness of the surfaces, the material itself and the type of lubricant or speed of movement between the surfaces that touch. The result of friction in the joints is the loss of energy and their heating, which ultimately leads to nonlinearities. For this reason, the creation of a dynamic friction model in joints is viewed as an important undesirable phenomenon that needs to be identified at the highest level [Hao 2021, Papageorgiou 2020].

The literature provides many created and mathematically defined models of friction, which serve to describe the given phenomenon and provide its mathematical formulations. Friction models are generally divided into two groups, namely static and dynamic models. A detailed overview of the respective models is given by the authors in the publications [Wang 2001, Harnoy 2008] and [Geffen 2009].

For static models, friction is a static function of velocity [Hao 2021]. This group includes, for example, Coulomb friction, which considers friction to be constant and depends on the direction of the velocity. A viscous friction model is also included here, in which the force is proportional to the speed. The authors in the publication [Hazem 2020] use a combination of the Coulomb and viscous model, referred to as the linear model, to identify the friction in the joints of the Triple Link Rotary Inverted Pendulum. The corresponding friction model was also applied by the authors in the publication [Fotuhi 2018] for the need to identify friction in the joints of the Laboratory 2-DOF Double Dual Twin Rotor Aero-dynamical System. The publication [Hao 2021] uses an extended friction model to identify friction in robot joints, which is based on the extended linear friction model and includes the Stribeck effect.

On the other hand, in dynamic models, the friction force does not only depend on the speed but also on the internal states, which also take into account the past samples of the friction force, not only the current state. Relevant examples of dynamic friction models are the Dahl model and the LuGre model. The relevant models describe friction based on the dynamic behaviour of the micro bristles of individual contact surfaces [Papageorgiou 2020]. The authors of the publication [Mashayekhi 2022] apply the LuGre model in friction research for a nonlinear and multi-DOF haptic device which is simplified to a 1-DOF. In the publication [Riill 2023], the LuGre model was defined and applied to research friction on a plane model of a festoon cable system. The individual mentioned static and dynamic friction models were applied in the process of identifying friction in the joints of the respective robotic manipulator with 3-DOF.

After designing the appropriate friction model, which will be used in the creation of a complete dynamic model, it is necessary to determine the values of its coefficients experimentally. After creating a simulation scheme in the Matlab Simulink environment, the individual coefficients are determined by comparing the measured and simulated curves of the angle of rotation of individual joints. Coefficient values are estimated using the Matlab program tool, namely the Parameter Estimator. An optimization method and an algorithm are used for estimations, which determine the sequence of steps in which the actual adjustment of the coefficient values takes place. The Trust-Region algorithm for non-linear least squares was applied for estimation [Santos 2014, Trojanova 2021].

The relevant article is divided into six chapters in total. The abstract is followed by an introduction that defines the current state of the problem being addressed. The next chapter is devoted to the description of the experimental system. The third chapter defines the designed friction models that were used within the complete dynamic model of the corresponding

manipulator. The theoretical parts are followed by a chapter dedicated to data collection for subsequent estimation and validation of the proposed friction models. The penultimate chapter describes the process of estimation and validation of the created models with the aim of determining the most optimal variant. At the end of the relevant article, its summary is given.

2 EXPERIMENTAL SYSTEM

The relevant article is focused on the estimation, validation, and comparison of the designed friction models in individual joints of an experimental manipulator with three degrees of freedom of movement, which is actuated by three pairs of FESTO fluidic muscles in an antagonistic connection. The experimental system itself consists of a support structure and a movable arm. The design of the manipulator is shown in Figure 1 [Cakurda 2022].

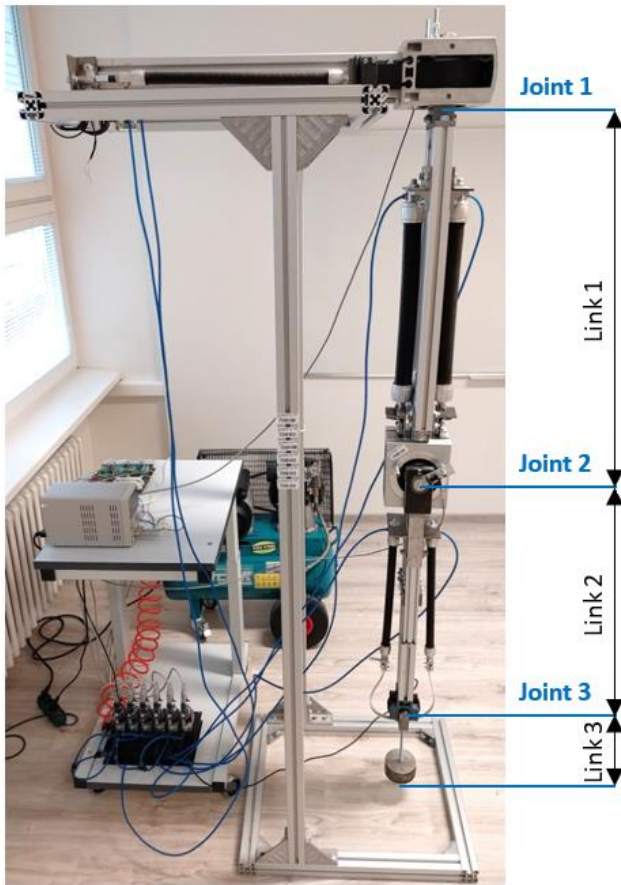


Figure 1. Experimental system

The behaviour of the real system is described by its complete dynamic model, which consists of a dynamic model of the basic functional elements, namely the dynamics of airflow, the dynamics of pressure and contraction of fluidic muscles, and the dynamics of the movement of individual arms. The dynamic model of the movement of the manipulator arms is expressed in a compact form by the nonlinear differential Equation 1, derived based on the Lagrange formalism [Ashagrie 2021]. The term $F(\dot{\theta})$ represents used friction models defined in the next chapter. [Cakurda 2022]

$$M(\theta)\ddot{\theta} + C(\theta, \dot{\theta})\dot{\theta} + G(\theta) + F(\dot{\theta}) = \tau \quad (1)$$

Figure 2 shows a 3D scheme of the experimental system, which represents the angular kinematic structure and shows the basic parameters of the manipulator, their location and designation. An overview of individual parameters and their definition are given in Table 1, where $i = 1, 2, 3$ [Cakurda 2022].

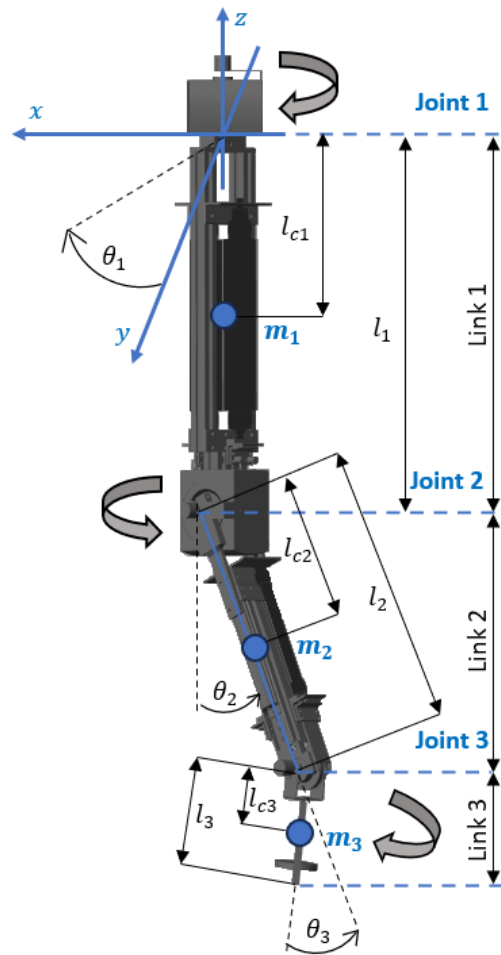


Figure 2. 3D scheme of experimental system

θ_i	Joint 1, 2, 3 angle
l_i	Link 1, 2, 3 length
m_i	Link 1, 2, 3 mass
l_{ci}	Link 1, 2, 3 centre of mass
I_{xi}	Link 2, 3 moment of inertia about axis x
I_{yi}	Link 2, 3 moment of inertia about axis y
I_{zi}	Link 1, 2, 3 moment of inertia about axis z

Table 1. Overview of 3D scheme parameters [Cakurda 2022]

3 MODELS USED TO IDENTIFY FRICTION IN THE MANIPULATOR'S JOINTS

In addition to the description of the dynamics of the movement of the arm itself and the dynamics of the used type of actuators, the dynamic model of the relevant investigated system also contains a dynamic model of friction in the individual joints of the manipulator. Friction in joints depends on speed and position [Geffen 2009]. For the analysis, identification and simulation of real processes, it is necessary to create a mathematical model of friction that adequately describes the friction in the joints of the manipulator. For friction identification, four different models were designed and used to describe friction in joints.

3.1 Linear friction model

The linear friction model belongs to the group of static models representing a function of velocity and position regardless of internal dynamics [Wang 2001]. The linear friction model

consists of a combination of Coulomb F_c and viscous F_v friction and is given by Equation 2 [Hazem 2019]:

$$F_l = F_c + F_v \quad (2)$$

Coulomb friction prevents relative motion and is proportional to the normal force. Coulomb friction is expressed by Equation 3, where f_{ci} for $i = 1, 2, 3$ represents the Coulomb friction coefficient for Joints 1, 2 and 3. The term $\dot{\theta}_i$ where $i = 1, 2, 3$ represents the angular velocity during the movement of the manipulator's joints. [Fotuhi 2018]

$$F_c = f_{ci} \text{sgn}(\dot{\theta}_i) \quad (3)$$

Viscous friction within the linear friction model is proportional to angular velocity and is expressed by Equation 4, where f_{vi} for $i = 1, 2, 3$ is the coefficient of viscous friction and $\dot{\theta}_i$, where $i = 1, 2, 3$ is the angular velocity [Fotuhi 2018]

$$F_v = f_{vi} \dot{\theta}_i \quad (4)$$

3.2 Extended friction model

The friction model described is one of the most used friction models. It is based on the extended Coulomb friction model and includes the Stribeck effect. Equation 5 represents the mathematical model that generalizes the linear friction model [Hao 2021]

$$F_{le} = f_{ci} \text{sgn}(\dot{\theta}_i) + f_{vi} \dot{\theta}_i + f_{1i} \dot{\theta}_i \text{sgn}(\dot{\theta}_i) + f_{2i} \dot{\theta}_i^3 \quad (5)$$

Coefficients f_{ci} and f_{vi} for $i = 1, 2, 3$ represent Coulomb and viscous friction coefficients, f_{1i} and f_{2i} for $i = 1, 2, 3$ are experimental friction coefficients, sgn represents a signum function and $\dot{\theta}_i$, where $i = 1, 2, 3$ is the angular velocity [Hao 2021, Hazem 2020].

3.3 Non-linear friction model

Friction in the joints of robotic manipulators is influenced by several factors, such as force, torque, position, speed, acceleration, or temperature. Due to the fact, that linear models cannot adequately describe the relevant characteristics, non-linear models are used to identify friction in manipulator joints. For research purposes, a non-linear model was used, which is expressed by Equation 6 and contains five different types of friction coefficients [Hazem 2020, Zhao 2020].

$$F_{nl} = f_{0i} + f_{ci} \text{sgn}(\dot{\theta}_i) + f_{vi} \dot{\theta}_i + f_{ai} \text{atan}(f_{bi} \dot{\theta}_i) \quad (6)$$

The definition of the coefficients f_{ci} and f_{vi} corresponds to the previous friction models, f_{ai} and f_{bi} are coefficients of the friction model obtained experimentally, f_{0i} is the zero-drift error of friction torque and $\dot{\theta}_i$ represents the angular velocity. For individual coefficients holds, that $i = 1, 2, 3$ [Hazem 2020].

3.4 LuGre model

The LuGre model is a dynamic friction model that describes the static and dynamic characteristics of friction. The name is derived from the universities of Lund and Grenoble, whose researchers designed the corresponding friction model. The model assumes that the contact surfaces consist of microscopic bristles and describes the dynamic effects of friction resulting from their defects. The LuGre friction model is expressed by Equation 7, where σ_0 is the stiffness of the contact bristles, σ_1 is the micro viscous coefficient, σ_2 is the viscous friction coefficient, and z represents the average value of the bristles bending [Mashayekhi 2022, Wang 2001].

$$F_{LG} = \sigma_0 z + \sigma_1 \dot{z} + \sigma_2 \dot{\theta} \quad (7)$$

The rate of bristle deflection \dot{z} is defined as [Mashayekhi 2022]:

$$\dot{z} = \dot{\theta} - \sigma_0 \frac{|\dot{\theta}|}{g(\dot{\theta})} z \quad (8)$$

where $g(\dot{\theta})$ represents the Stribeck effect, which is expressed by Equation 9 [Mashayekhi 2022]

$$g(\dot{\theta}) = F_c + (F_s - F_c) e^{-\left|\frac{\dot{\theta}}{v_s}\right|^2} \quad (9)$$

The term F_c represents the Coulomb friction force, F_s the stiction force, v_s the Stribeck velocity and $\dot{\theta}$ the angular velocity.

4 MEASURED DATA

The data required for the estimation and validation of the designed friction models in the joints of the manipulator were obtained based on the measurements. The angles of rotation of individual joints were monitored during the measurements. During the measurements, the arms were driven using three pairs of FESTO fluidic muscles in antagonistic connection. The selected method of excitation was secured using the Matlab Simulink program tool, namely Signal Builder. The measurements consisted of the initial pressurization of the fluidic muscles to a set pressure value and subsequently deflated and pressurized one of the pair of fluidic muscles. Under the specified conditions, ten measurements were made and then the average courses of the rotation angle of the joints were obtained based on the measurements, which were compared with the output of the model.

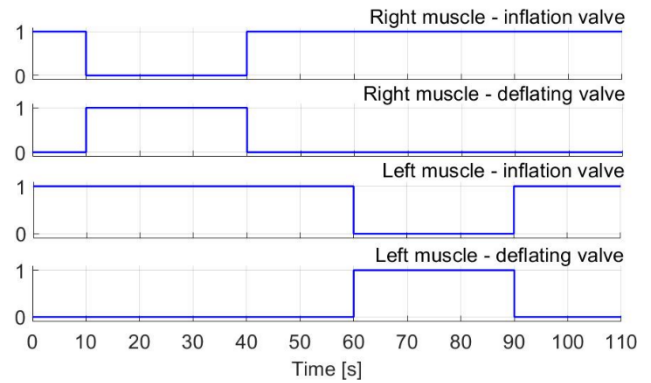


Figure 3. Control signal for Joint 1 fluidic muscles

Figure 3 shows the control signal for the driving of the upper pair of fluidic muscles driving Joint 1. The control signal consisted of initially pressurizing the pair of muscles to a value of 550 kPa. In the tenth second, the right muscle was deflated by 350 kPa and repressurized in the fortieth second of the measurement. The left muscle was deflated at the sixtieth second by 400 kPa and pressurized to the initial value at the ninetieth second. Ten measurements were made under the specified conditions. The average course of the rotation angle of Joint 1 is shown in Figure 4.

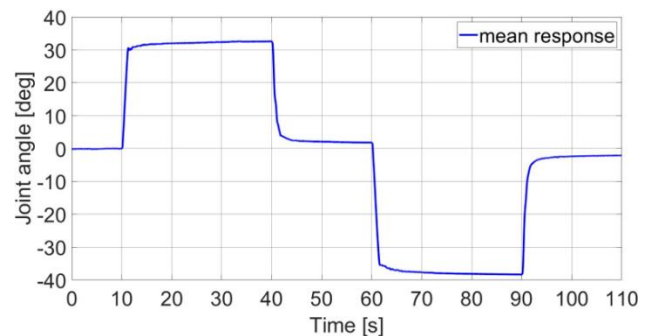


Figure 4. The average course of the angle of Joint 1

The control signal for another pair of fluidic muscles driving Joint 2 is shown in Figure 5. After pressurizing the muscles to 550 kPa, the left muscle was deflated by 350 kPa at the tenth second and repressurized at the fortieth second. In the sixtieth second, the right muscle was deflated by 300 kPa and its pressurization followed in the ninetieth second. The average course of the rotation angle of Joint 2 is shown in Figure 6.

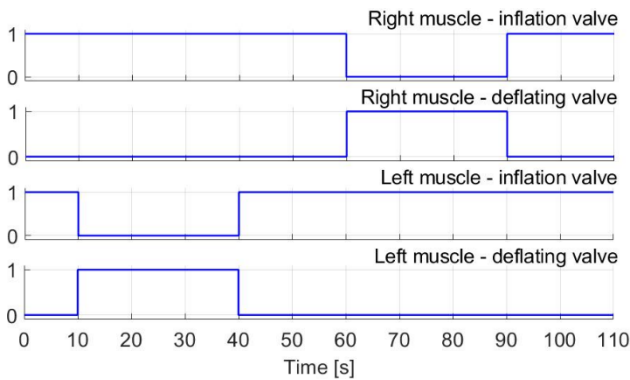


Figure 5. Control signal for Joint 2 fluidic muscles

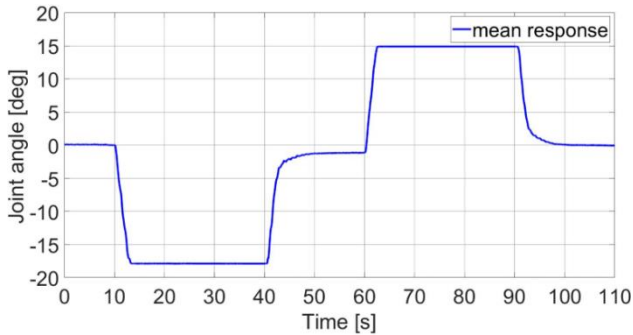


Figure 6. The average course of the angle of Joint 2

The control signal for the lower pair of fluidic muscles that drives Joint 3 corresponds to the control signal for Joint 1, which is shown in Figure 3. The time intervals for deflating and pressurizing the fluidic muscles and the pressure value correspond to the excitation method for Joint 1. The average course of the rotation angle of Joint 3 is shown in Figure 7.

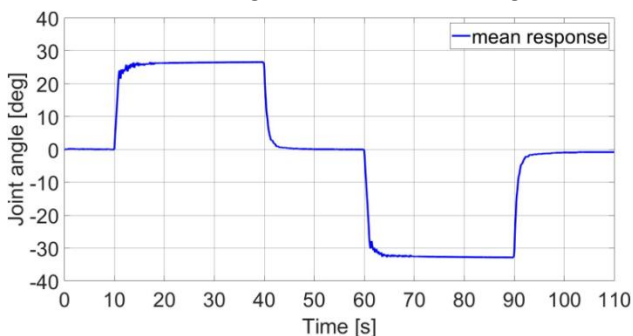


Figure 7. The average course of the angle of Joint 3

5 ESTIMATION AND VALIDATION OF DESIGNED FRICTION MODELS

Estimation and validation of the designed friction models took place in the Matlab Simulink program, where a simulation scheme was created for the dynamic model of the experimental manipulator, including the friction models. Individual parameters of the dynamic model were obtained based on measurements and from the 3D CAD model. The parameter values are shown in Table 2. In the estimation process, the coefficients of the designed friction models were modified based on the comparison of the simulated and measured course of the

angle of rotation of the individual joints. To estimate the coefficients of the relevant friction models, the tool of the Matlab program, namely the Parameter Estimator, was used.

Symbol	Value	Unit
l_2	0.8100	m
l_{c2}	0.5050	m
l_{c3}	0.1943	m
m_2	11.895	kg
m_3	4.7538	kg
I_{x2}	0.0798	kg.m ²
I_{x3}	0.0654	kg.m ²
I_{y2}	0.0031	kg.m ²
I_{y3}	0.0420	kg.m ²
I_{z1}	0.0014	kg.m ²
I_{z2}	0.0035	kg.m ²
I_{z3}	0.0910	kg.m ²

Table 2. Parameter values of dynamic model

During the validation process, the output of the model and the measured courses of the angle of rotation of individual joints were compared based on the statistical indicators RMSE (Root Mean Square Error) and SSE (Sum Square Error). RMSE is a general error estimate that determines the average difference between the predicted (simulated) values and the actual (measured) values. The relevant indicator provides an estimate of the level at which the created model is capable of simulating the required value. Its calculation is given by Equation 10, where y_{mi} represents the measured value, y_{pi} is the simulated value and n is the number of samples. In general, the lower the value of the RMSE indicator, the more accurate the created model is. [Lodetti 2022]

$$RMSE = \sqrt{\frac{1}{n} \sum_{i=1}^n (y_{mi} - y_{pi})^2} \quad (10)$$

SSE represents an indicator that expresses the error as the sum of the squares of the difference between the measured value y_{mi} and the simulated value y_{pi} . The value of the SSE indicator is determined based on Equation 11, and the lower its value, the smaller the variability of the model output compared to the measured values. [Pham 2019]

$$SSE = \sum_{i=1}^n (y_{mi} - y_{pi})^2 \quad (11)$$

5.1 Estimation and validation of the linear friction model

In the process of estimating the linear friction model, it was necessary to determine the values of the respective coefficients f_{ci} and f_{vi} . Their original value was set to 0.1. The bounds of the searched values of the coefficients were set in the interval from 0.001 to 10. Based on the performed estimation, we received the modified values of the coefficients, which are listed in Table 3.

Symbol	Value	Unit	Symbol	Value	Unit
f_{c1}	0.0376	N.m.s.rad ⁻¹	f_{v2}	3.3254	N.m
f_{v1}	1.5473	N.m	f_{c3}	0.0512	N.m.s.rad ⁻¹
f_{c2}	0.1446	N.m.s.rad ⁻¹	f_{v3}	0.1537	N.m

Table 3. Coefficient values of the linear friction model

The results of the validation of the dynamic model with the linear friction model based on selected statistical indicators are presented in Table 4.

Joint 1	RMSE	3.0610
	SSE	$1.0306 \cdot 10^6$
Joint 2	RMSE	1.2341
	SSE	$1.6754 \cdot 10^5$
Joint 3	RMSE	1.8602
	SSE	$3.8063 \cdot 10^5$

Table 4. Results of validation for the linear friction model

The lowest value of the statistical indicator RMSE was achieved by the course of rotation of Joint 2, namely $RMSE = 1.2341$, and the highest value, i.e. $RMSE = 3.0610$, was achieved for Joint 3. Within the SSE indicator, the limit values were $1.6754 \cdot 10^5$ for Joint 2 and $1.0306 \cdot 10^6$ for Joint 1. A comparison of the rotation angle curves of individual joints is shown in Figure 8, Figure 9 and Figure 10.

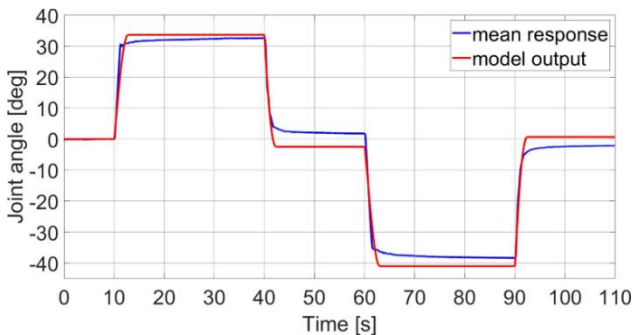


Figure 8. Model and system output for Joint 1

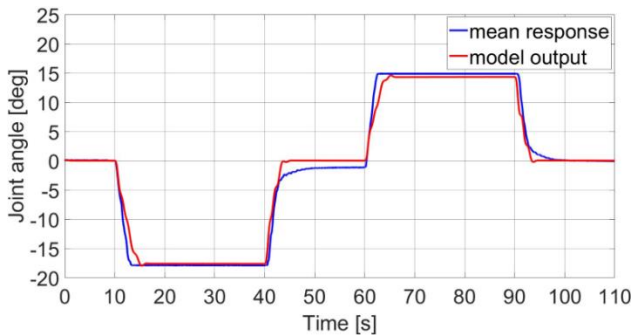


Figure 9. Model and system output for Joint 2

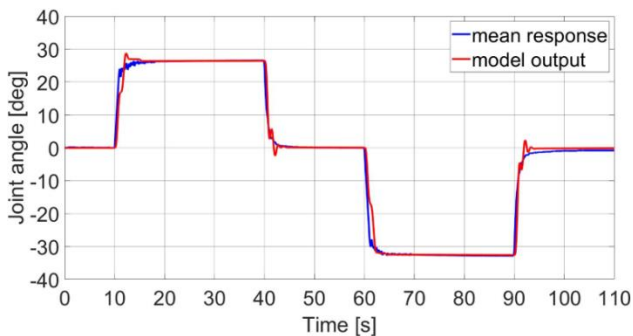


Figure 10. Model and system output for Joint 3

5.2 Estimation and validation of the extended friction model

The estimation of the extended friction model was aimed at determining the values of its individual coefficients f_{ci} , f_{vi} , f_{1i} and f_{2i} . The original value of the searched coefficients and their

bounds for estimation corresponded to the linear friction model. The values of the coefficients of the relevant friction model, which were obtained on the basis of the performed estimation, are shown in Table 5.

Symbol	Value	Unit	Symbol	Value	Unit
f_{c1}	0.2195	N.m.s.rad ⁻¹	f_{12}	3.1062	N.m.s.rad ⁻¹
f_{v1}	0.0800	N.m	f_{22}	0.1126	N.m
f_{11}	0.9084	N.m.s.rad ⁻¹	f_{c3}	0.0233	N.m.s.rad ⁻¹
f_{21}	6.3584	N.m	f_{v3}	0.0101	N.m
f_{c2}	0.0824	N.m.s.rad ⁻¹	f_{13}	0.2301	N.m.s.rad ⁻¹
f_{v2}	3.2338	N.m	f_{23}	0.0538	N.m

Table 5. Coefficient values of the extended friction model

Table 6 shows the results of the validation process of the extended friction model based on the statistical indicators Root Mean Square Error and Sum Square Error.

Joint 1	RMSE	1.7812
	SSE	$3.4900 \cdot 10^5$
Joint 2	RMSE	1.1192
	SSE	$1.3778 \cdot 10^5$
Joint 3	RMSE	1.7403
	SSE	$3.3114 \cdot 10^5$

Table 6. Results of validation for the extended friction model

The value of the indicator $RMSE = 1.1192$ for Joint 2 represents its best value, and the value of $RMSE = 1.7812$ for Joint 1, on the other hand, is the worst value. Within the second proposed indicator, the lowest value of $SSE = 1.3778 \cdot 10^5$ was also achieved for Joint 2, and the highest value of $SSE = 3.4900 \cdot 10^5$ was obtained for the angle of rotation of Joint 1. The comparison of the courses of the angle of rotation of individual joints is shown in Figure 11, Figure 12 and Figure 13.

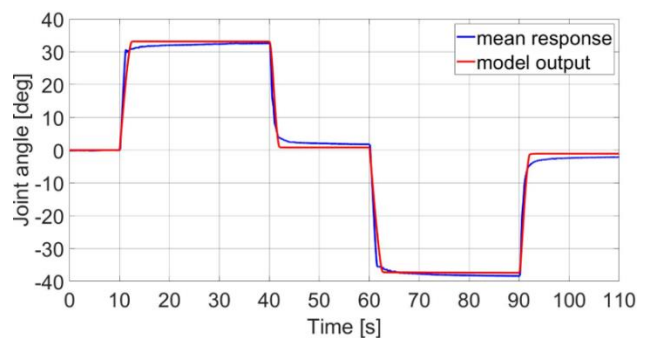


Figure 11. Model and system output for Joint 1

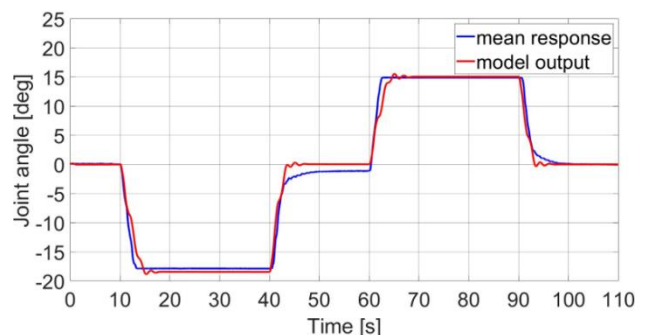


Figure 12. Model and system output for Joint 2

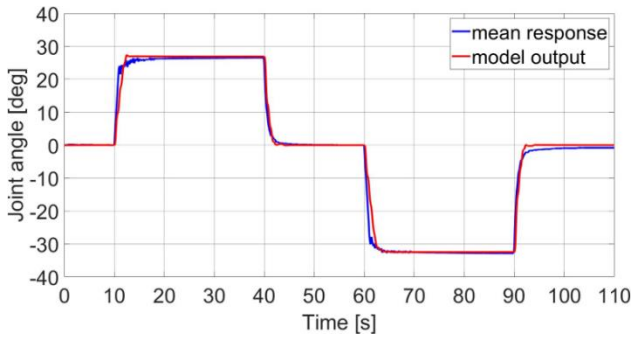


Figure 13. Model and system output for Joint 3

5.3 Estimation and validation of a non-linear friction model

The estimation of the non-linear friction model, as in the previous two cases, was aimed at determining the relevant coefficients for individual joints, namely f_{0i} , f_{ci} , f_{vi} , f_{ai} and f_{bi} . Likewise, the bounds of the searched coefficients were set in the range of 0.001 to 10, and their original value was 0.1. The resulting values of the coefficients of the nonlinear friction model are shown in Table 7.

Symbol	Value	Unit	Symbol	Value	Unit
f_{01}	0.0025	N.m	f_{a2}	1.8990	N.m.s.rad ⁻¹
f_{c1}	0.0034	N.m.s.rad ⁻¹	f_{b2}	1.1963	N.m
f_{v1}	1.5019	N.m	f_{03}	0.0649	N.m
f_{a1}	1.2325	N.m.s.rad ⁻¹	f_{c3}	0.0338	N.m.s.rad ⁻¹
f_{b1}	0.1889	N.m	f_{v3}	0.0078	N.m
f_{02}	0.2391	N.m	f_{a3}	0.0523	N.m.s.rad ⁻¹
f_{c2}	0.0045	N.m.s.rad ⁻¹	f_{b3}	0.8921	N.m
f_{v2}	3.0809	N.m			

Table 7. Coefficient values of the non-linear friction model

The results of the validation of the dynamic model based on the statistical indicators Root Mean Square Error and Sum Square Error, in which a non-linear model was used for the friction in the joints, are shown in Table 8.

Joint 1	RMSE	2.2694
	SSE	5.6654*10 ⁵
Joint 2	RMSE	1.1368
	SSE	1.4216*10 ⁵
Joint 3	RMSE	1.8252
	SSE	3.6646*10 ⁵

Table 8. Results of validation of the non-linear friction model

The RMSE indicator with a value equal to 1.1368 for Joint 2 represented its lowest value, and RMSE = 2.2694 for Joint 1, on the other hand, its highest value. The resulting values of the SSE indicator ranged from 1.4216*10⁵ for Joint 2, which represented its best value, to 5.6654*10⁵ for Joint 1, which represented its worst value. Figures 14, 15 and 16 show comparisons of the simulated and measured curves of the rotation angle of individual joints.

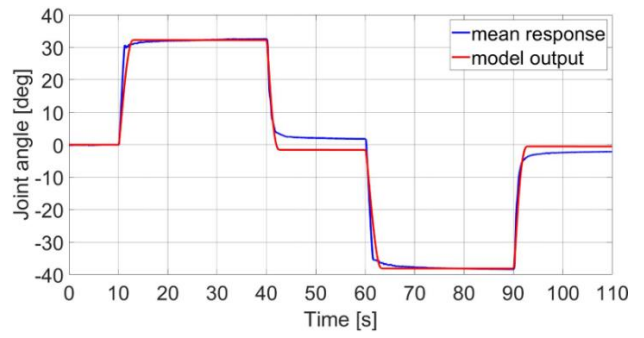


Figure 14. Model and system output for Joint 1

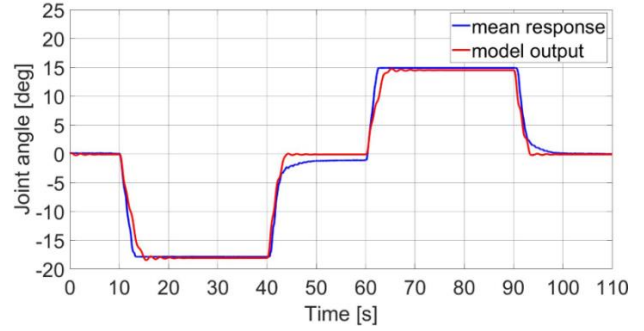


Figure 15. Model and system output for Joint 2

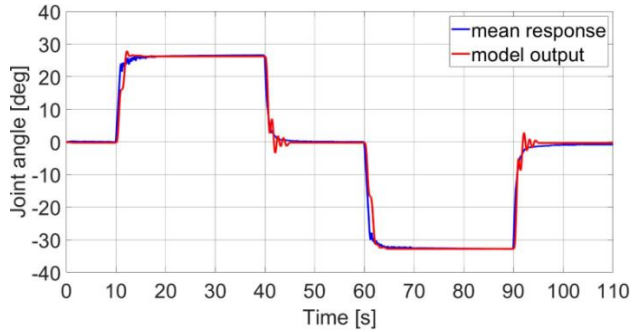


Figure 16. Model and system output for Joint 3

5.4 Estimation and validation of the LuGre model

The LuGre model was the last designed friction model for the identification of friction in the individual joints. As in the previous friction models, in the estimation process, we determined the values of its coefficients, i.e. σ_{0i} , f_{ci} , f_{si} , v_{si} , σ_{1i} , σ_{2i} and z_i . Limitations and original coefficient values remained unchanged. The resulting values of the LuGre coefficients of the friction model are shown in Table 9.

Symbol	Value	Unit	Symbol	Value	Unit
σ_{01}	0.0153	N.m ⁻¹	σ_{12}	3.9920	N.s.m ⁻¹
f_{c1}	1.5018	N.m.s.rad ⁻¹	σ_{22}	2.5832	N.s.m ⁻¹
f_{s1}	1.6532	N.m	z_2	2.6*10 ⁻⁶	m
v_{s1}	0.7524	m.s ⁻¹	σ_{03}	0.0999	N.m ⁻¹
σ_{11}	0.1000	N.s.m ⁻¹	f_{c3}	0.4170	N.m.s.rad ⁻¹
σ_{21}	1.8068	N.s.m ⁻¹	f_{s3}	6.4911	N.m
z_1	8.8*10 ⁻⁶	m	v_{s3}	4.0947	m.s ⁻¹
σ_{02}	0.0314	N.m ⁻¹	σ_{13}	0.0077	N.s.m ⁻¹
f_{c2}	0.0783	N.m.s.rad ⁻¹	σ_{23}	0.1072	N.s.m ⁻¹
f_{s2}	0.9187	N.m	z_3	0.2*10 ⁻⁶	m
v_{s2}	0.6895	m.s ⁻¹			

Table 9. Coefficient values of the LuGre model

Table 10 shows the results of the LuGre friction model validation process based on the statistical indicators Root Mean Square Error and Sum Square Error.

Joint 1	RMSE	2.2930
	SSE	$5.7835 \cdot 10^5$
Joint 2	RMSE	1.3597
	SSE	$2.0335 \cdot 10^5$
Joint 3	RMSE	1.5891
	SSE	$2.7777 \cdot 10^5$

Table 10. Results of validation of the LuGre model

Based on the performed validation, we can see that the smallest variability compared to the measured values was achieved by the LuGre model for Joint 2, namely $RMSE = 1.3597$ and $SSE = 2.0335 \cdot 10^5$. The respective values of the proposed statistical indicators represent their lowest value. On the other hand, $RMSE = 2.2930$ and $SSE = 5.7835 \cdot 10^5$ for Joint 1 represented the highest values of the given indicators and thus the greatest variability of the LuGre model compared to the measured data. The comparison of the courses of the angle of rotation of individual joints is shown in Figure 17, Figure 18 and Figure 19.

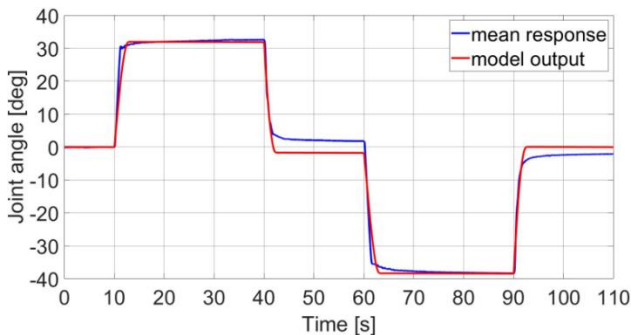


Figure 17. Model and system output for Joint 1

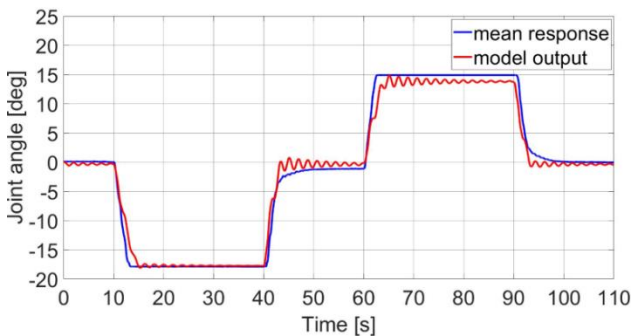


Figure 18. Model and system output for Joint 2

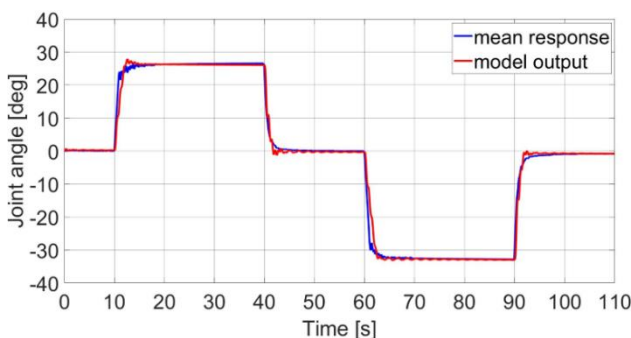


Figure 19. Model and system output for Joint 3

6 CONCLUSIONS

The relevant article was focused on the research of friction in individual joints of an experimental manipulator with three degrees of freedom of movement, which is actuated by three pairs of FESTO fluidic muscles in an antagonistic connection. Four models were proposed to identify the friction, which were used within the complete dynamic model of the experimental system. For the dynamic model of the system and the friction models, a simulation scheme was created in the Matlab Simulink program, which was used for subsequent estimation and validation. The estimation of the friction models consisted of adjusting their individual coefficients using the Parameter Estimator tool, based on the comparison of the measured and simulated course of the angle of rotation of the individual joints of the manipulator. The estimation was followed by a validation process, where the output of the model and the system were compared based on the proposed statistical indicators, namely RMSE (Root Mean Square Error) and SSE (Sum Square Error).

Within the validation of the movement of Joint 1, the best value of the RMSE indicator = 1.7812 was achieved by the extended friction model, and the worst value was the $RMSE = 3.0610$ by the linear friction model. The SSE indicator showed the lowest value $SSE = 3.4900 \cdot 10^5$ also for the extended friction model and the highest value $SSE = 1.0306 \cdot 10^6$ similarly for the linear friction model.

The validation of the models describing the friction during the movement of Joint 2 showed that the best value of the RMSE indicator was achieved as in the case of Joint 1 when using the extended friction model, namely $RMSE = 1.1192$. Unlike Joint 1, the worst value of the RMSE indicator = 1.3597 was achieved when using the LuGre model. The second used indicator reached the best value also when using the extended friction model, namely $SSE = 1.3778 \cdot 10^5$ and the worst value when using the LuGre model, i.e. $SSE = 2.0335 \cdot 10^5$.

The validation of the friction models based on the comparison of the outputs of the model and the system for Joint 3 showed that the LuGre model showed the lowest value of the RMSE indicator, namely $RMSE = 1.5891$, and the highest was the linear model, i.e. $RMSE = 1.8602$. For the SSE indicator, the best SSE value = $2.7777 \cdot 10^5$ again when using the LuGre model and the worst SSE value = $3.8063 \cdot 10^5$ when using the linear model.

The validation results showed that the linear friction model achieved the worst values of the RMSE and SSE indicators for all joints. On the other hand, the best indicator values for Joint 1 and Joint 2 were obtained when using the extended friction model. For Joint 3, the best results were achieved when using the LuGre model, but the graphic curves show larger oscillations than when using the extended model, which for Joint 3 achieved the second-best values of RMSE and SSE indicators. Considering the presented results, the extended friction model represents the best variant for the identification of friction in the joints of the experimental manipulator.

ACKNOWLEDGMENTS

This research was funded by the project VEGA 1/0061/23, "Research of modeling and control of soft continuum arms based on fluidic muscles using bio-inspired computational methods" (Slovak Republic).

REFERENCES

- [Ashagrie 2021] Ashagrie, A., et al. Modeling and control of a 3-DOF articulated robotic manipulator using self-tuning fuzzy sliding mode controller. *Cogent Engineering*, 2021, Vol. 8, No. 1, p. 33.
- [Cakurda 2022] Cakurda, T., et al. Complete Dynamic Model Validation of 3-DOF Compliant Manipulator with Fluidic Muscles. *MM Science Journal*, 2022, No. December, pp. 6139-6146.
- [Fotuhi 2018] Fotuhi, M.J., et al. Comparison of Joint Friction Estimation Models for Laboratory 2 DOF Double Dual Twin Rotor Aero-dynamical System. In: *IECON 2018 - 44th Annual Conf. of the IEEE Industrial Electronics Society*. Washington, 21-23 October 2018. New York: IEEE, pp. 2231-2236. ISBN 978-1-5090-6684-1.
- [Garabin 2020] Garabin, G., Scalera, L. On the Trajectory Planning for Energy Efficiency in Industrial Robotic Systems. *Robotics*, 2020, Vol. 11, No. 4, pp. 1-13.
- [Geffen 2009] Geffen, V. A study of friction models and friction compensation. Technische Universiteit Eindhoven, 2009, Eindhoven. [Online]. [12.09.2023]. Available from <<http://coccweb.cocc.edu/bemerson/PhysicsGlobal/Courses/PH211/PH211Materials/PH211Breadcrumb/BreadcrumbDocuments/FrictionGeneral.pdf>>.
- [Hao 2021] Hao, L., et al. Dynamic and Friction Parameters of an Industrial Robot: Identification, Comparison and Repetitiveness Analysis. *Robotics*, 2021, Vol. 10, No. 1, pp. 1-17.
- [Harnoy 2008] Harnoy, A., et al. Modeling and measuring friction effects. *IEEE Control Systems Magazine*, 2008, Vol. 28, No. 6, pp. 82-91.
- [Hazem 2019] Hazem, Z.B., et al. Comparison of Friction Estimation Models for Rotary Triple Inverted Pendulum. *Int. J. of Mechanical Eng. and Robotics Research*, 2019, Vol. 8, No. 1, pp. 74-78.
- [Hazem 2020] Hazem, Z. B., et al. A Comparative Study of the Joint Neuro-Fuzzy Friction Models for a Triple Link Rotary Inverted Pendulum. *IEEE Access*, 2020, Vol. 8, pp. 49066-49078. ISSN 2169-3536.
- [Lodetti 2022] Lodetti, P. Z., et al. MAE and RMSE Analysis of K-means Predictive Algorithm for Photovoltaic Generation. In: *2022 Int. Conf. on Electrical, Computer and Energy Technologies (ICECET)*, Prague, 20-22 July, 2022. New Jersey: IEEE Explore, pp. 1-6. ISBN 978-1-6654-7087-2.
- [Mashayekhi 2022] Mashayekhi, A., et al. Analytical describing function of LuGre friction model. *Int. J. of Intelligent Robotics and Applications*, 2022, Vol. 6, No. 1, pp. 437-448.
- [Matheson 2019] Matheson, E., et al. Human-Robot Collaboration in Manufacturing Applications: A Review. *Robotics*, 2019, Vol. 8, No. 4, pp. 1-28.
- [Papageorgiou 2020] Papageorgiou, D., et al. Online friction parameter estimation for machine tools. *Advanced Control for Applications: Engineering and Industrial Systems*, 2020, Vol. 2, No. 1, pp. 1-27.
- [Pham 2019] Pham, H. A New Criterion for Model Selection. *Mathematics*, 2019, Vol. 7, No. 12, pp. 1-12.
- [Rill 2023] Rill, G., Schuderer, M. A Second-Order Dynamic Friction Model Compared to Commercial Stick-Slip Models. *Modelling*, 2023, Vol. 4, No. 3, pp. 366-381.
- [Santos 2014] Santos, S.A. Trust-Region-Based Methods for Nonlinear Programming: Recent Advances and Perspectives. *Pesquisa Operacional*, September 2014, Vol. 34, No. 3, pp. 447-462. ISSN 1678-5142.
- [Trojanova 2023] Trojanova, M., et al. Evaluation of Machine Learning-Based Parsimonious Models for Static Modeling of Fluidic Muscles in Compliant Mechanisms. *Mathematics*, 2023, Vol. 11, No. 1, pp. 1-33.
- [Wang 2001] Wang J., et al. Adaptive Friction Compensation for Servo Mechanisms. In: *Adaptive Control of Nonsmooth Dynamic Systems*. London: Springer-Verlag London Ltd., 2001. ISBN 978-1-85233-384-3.
- [Zhao 2020] Zhao, L., et al. Nonlinear friction dynamic modeling and performance analysis of flexible parallel robot. *Int. J. of Adv. Robotic Systems*, 2020, Vol. 17, No. 6, pp. 1-14. ISSN 1729-8814.

CONTACTS

Ing. Tomas Cakurda, PhD.

Ing. Monika Trojanova, PhD.

Assoc. Prof. Ing. Alexander Hosovsky, PhD.

Ing. Pavlo Pomin

Technical University of Kosice

Faculty of Manufacturing Technologies with the Seat in Presov

Department of Industrial Engineering and Informatics

Bayerova 1, 080 01 Presov, Slovakia

+421 055 602 6420

tomas.cakurda@tuke.sk, monika.trojanova@tuke.sk, alexander.hosovsky@tuke.sk, pavlo.pomin@tuke.sk